ZIF-8@PBI-BuI composite membranes: Eloquent effects of PBI structural variation towards gas permeation performance

(Supporting Information)

Anand Bhaskar,[a] Rahul Banerjee*[b] and UlhasKharul*[a]

[a]Polymer Science and Engineering Division, CSIR-National Chemical Laboratory,
Dr. Homi Bhabha Road, Pune - 411008, India.
Fax: 020-25902618; Tel: 020-25902180; E-mail: uk.kharul@ncl.res.in.

[b]Physical Chemistry Division, CSIR-National Chemical Laboratory,
Dr. Homi Bhabha Road, Pune - 411008, India.
Fax: 020-25902636; Tel: 020-25902535; E-mail: r.banerjee@ncl.res.in

Section S1:Synthesis and characterization of ZIF-8

(a) Synthesis of ZIF-8

The ZIF-8 nanocrystals were synthesized by following a reported method.[1] A solution of 2-methylimidazole (16.22 g, 0.197 mol) was prepared in 500 ml of methanol. A separate solution of $Zn(NO_3)_2 \cdot 6H_2O$ (7.33 g, 0.024 mol) in 500 ml of methanol was prepared. Both, the legand and metal ion solutions were mixed together and stirred for an hour. It was then centrifuged and the sediment was collected. It was washed twice with 250 ml of DMAc and then dispersed in 200 ml of DMAc while stirring and sonicating four times (10 min for each cycle, with an interval of 1 h, while stirring). This protocol resulted into a suspension which remained stable for several days. This was used as a stock suspension for further use. Its concentration was determined by taking two samples of 10 ml each and removing solvent by evaporation followed by vacuum drying at 100 °C for a day.

(b) Characterizationof synthesized ZIF-8

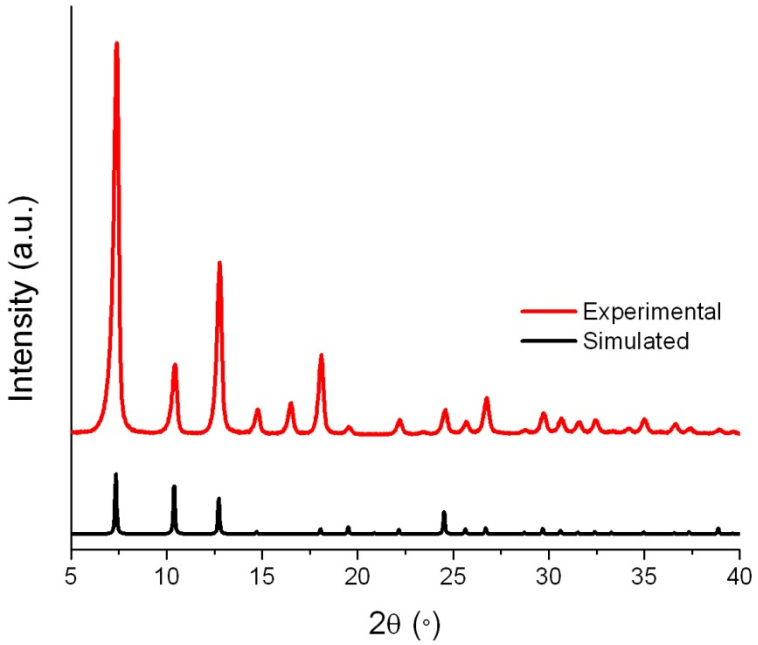

Fig. S1 XRD spectra of ZIF-8 compared with simulated data. The experimental data correlates well with the simulated one.

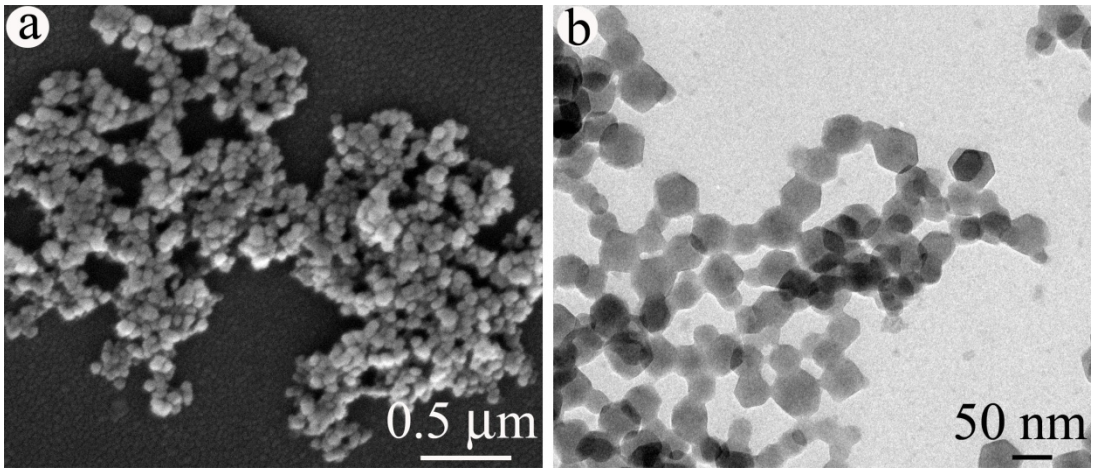

Fig. S2 SEM image (a) and TEM image (b) of ZIF-8

SEM and TEM images showsmall size distribution of ZIF-8 nanoparticles (60-80 nm). In TEM image of ZIF-8 nanoparticles rhombic dodecahedron shapes are visible.

Section S2: Synthesis and characterization of PBI-BuI and its *N*-substitution

(a) Synthesis of PBI-BuI

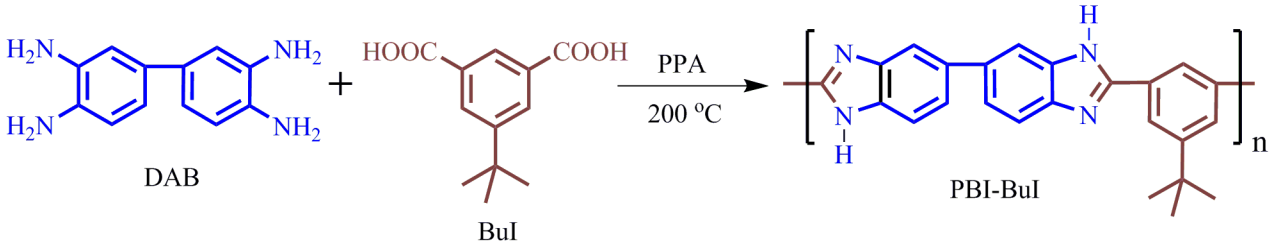

Scheme S1. Synthesis of PBI-BuI

The PBI-BuI was synthesized by solution polycondensation of 3,3′-diaminobenzidine (DAB) and 5-*tert*-butylisophthalic acid (BuI) in polyphosphoric acid (PPA) (Scheme S1) as reported earlier.[2] In a typical procedure, the DAB (40.007 g, 0.18671 mol) was dissolved in PPA (1200 g) at 140 ºC under inert atmosphere. The BuI (41.494 g, 0.18671 mol) was added; temperature was raised to 170 ºC and maintained for 5 h. The temperature was further raised to 210 ºC and maintained for further 12 h. Obtained viscous reaction mixture was poured on to the stirred water. The precipitated polymer was crushed and thoroughly washed with water till the filtrate was neutral to pH. The polymer was then kept overnight in saturated aqueous $NaHCO_3$ solution, washed with water until neutral to pH and soaked in acetone for 16 h in order to extract the water from polymer matrix. The dried polymer (100 ºC, 7 days) was further purified by dissolving in DMAc (2.5% w/v), removing undissolved particles, if any, by centrifugation at 3000 rpm for 3 h and reprecipitation on to the stirred water. The polymer was finally dried at 60 °C for 24 h and then in vacuum oven at 100 °C for a week.

(b) *N*-substitution of PBI-BuI

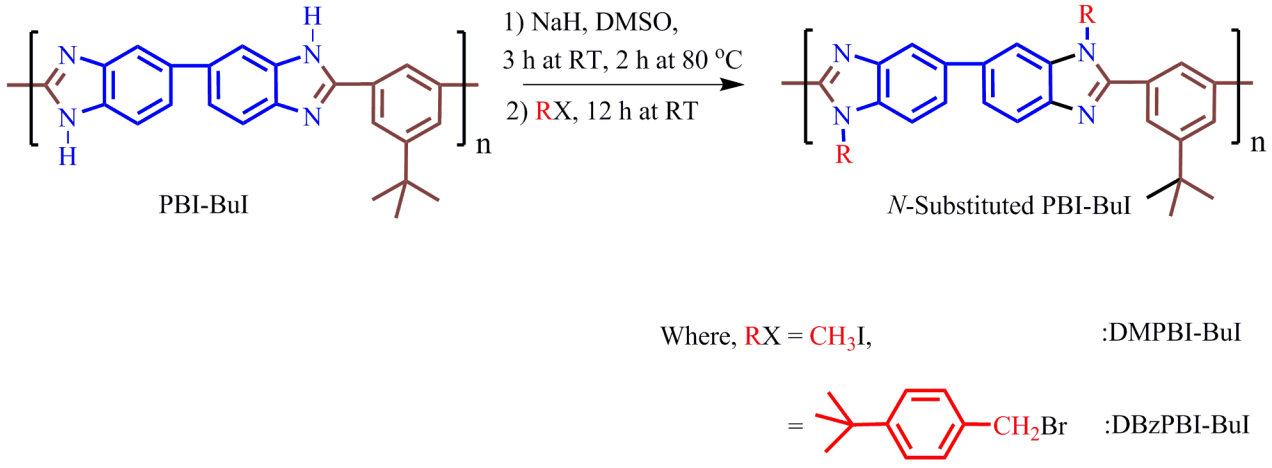

Scheme S2. *N*-Substitution of PBI-BuI

The *N*-substitution reaction of PBI-BuI (Scheme S2) was carried out as reported earlier.[3] Typically, in a three-necked round-bottomed flask, PBI-BuI (10.0 g, 0.0275 mol) was dissolved in 300 ml of dry DMSO and 2.1 equivalents of NaH (2.31 g, 0.0576 mol, 60% dispersion in mineral oil) was added under inert atmosphere. The solution was stirred at ambient for 3 h and

then at 80 °C for 2 h. The reaction mixture was cooled to the ambient and 2 molar equivalents of alkyl halide (methyl iodide or 4-*tert*-butylbenzyl bromide dissolved in 10 ml of dry DMSO) were added in a drop wise manner for a period of 15 min. The reaction mixture got precipitated indicating formation of the *N*-substituted PBI. It was stirred further at ambient temperature for 12 h and precipitated in acetone. Obtained polymer was separated and vacuum dried at 100 °C for 3 days. It was further purified by dissolving in DMAc and reprecipitation in acetone.

(c) Characterization of synthesized polymers

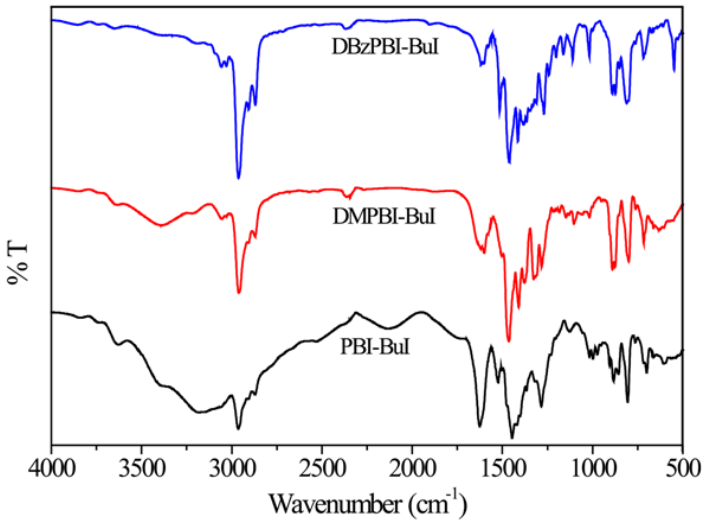

Fig. S3 FTIR spectra of polymers

The Inherent viscosity (η_{inh}) of PBI-BuI and *N*-substituted PBIs was determined using their DMAc solution (0.2 g/dL) at 35 °C. The inherent viscosity of PBI-BuI, DMPBI-BuI and DBzPBI-BuI was 0.84, 0.99 and 0.71dL/g respectively. The FTIR spectra of all three polymers are given in Fig. S4 (recorded using Perkin Elmer Spectrum GX spectrophotometer).The characteristic peaks of benzimidazole ring at 1430, 1600, and 1620 cm^{-1} confirmed completion of the imidazole ring formation during PBI synthesis. The positioning of other bands also matched with those reported previously. FTIR spectra (Fig. S4) of *N*-substituted PBIs, show no broad peak at 3140 cm^{-1}. This confirms substitution of imidazole hydrogen by alkyl group. In the FTIR spectra of all three polymers, peaks for free O-H stretching and O-H…N stretching are also observed at 3648 cm^{-1} and 3420 cm^{-1} respectively due to trace of absorbed moisture.[4]

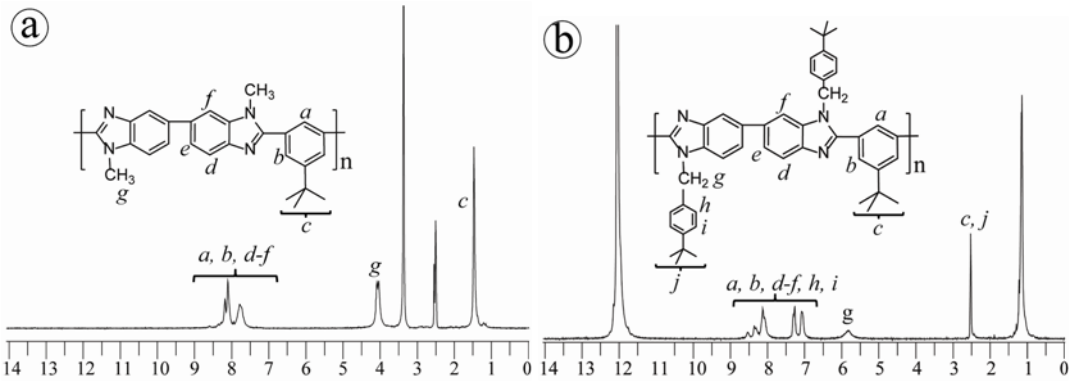

Fig. S4 NMR spectra of (a) DMPBI-BuI and (b) DBzPBI-BuI.

The ^{1}H-NMR spectra of *N*-substituted polymers showed no peak for N-H proton, which is further confirmation of quantitative substitution. The ^{1}H-NMR spectra of DMPBI-BuI (Fig.S5a) show peaks at 7.78-8.18 ppm for aromatic protons, 4.04 ppm for methyl protons and at 1.47 ppm for *tert*-butyl protons. The ^{1}H-NMR spectra of DBzPBI-BuI (Fig. S5b) show peaks at 7.08-8.54 ppm for aromatic protons, 5.83 ppm for methylene protons and at 1.14 ppm for protons belonging to *tert*-butyl groups. The degree of substitution for DMPBI-BuI was calculated by comparing integration of methyl group protons with that of aromatic protons. In case of DBzPBI-BuI, comparison of aromatic protons of the substituent group with the aromatic protons of PBI-BuI backbone was made. It was found to be 99.3% and 100% for DMPBI-BuI and DBzPBI-BuI, respectively. WAXD pattern of DMPBI-BuI and DBzPBI-BuI showed broad amorphous hollow at 2θ value of 19.11° and 16.69°, respectively.

Section S3: Elemental mapping, physical properties and gas permeation properties of composite membranes

(a) Elemental mapping

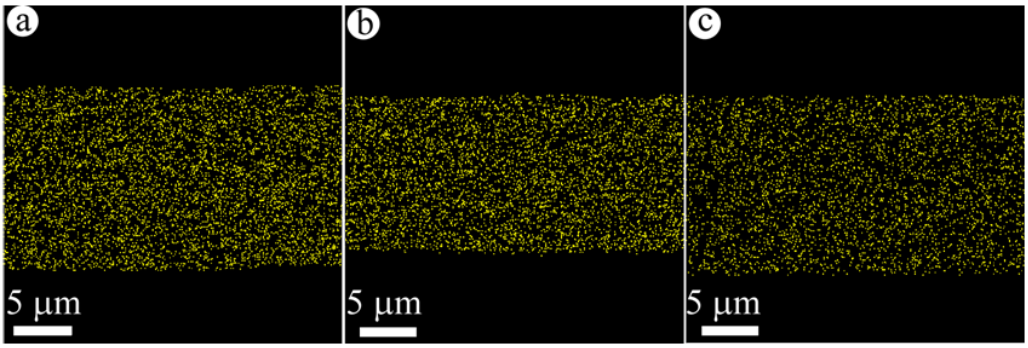

Fig. S5 Zn mapping of (a) Z_{30}@PBI-BuI, (b) Z_{30}@DMPBI-BuI and (c) Z_{20}@DBzPBI-BuI composite membranes.

Elemental mapping of the ZIF-8 based composite membranes (Fig. S5) shows even distribution of Zn throughout the width of the respective membrane. This proves that both types of composite membranes have homogeneous distribution of MOF throughout the membrane thickness.

(b) Thermo gravimetric analysis of membranes

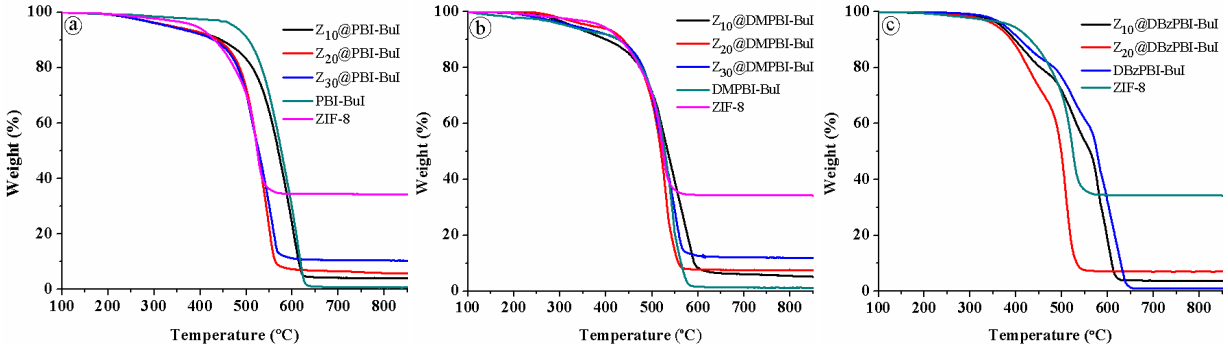

Fig. S6 TGA thermograms of PBIs, ZIF-8 and composites: (a) PBI-BuI, ZIF-8 and their composites, (b) DMPBI-BuI, ZIF-8 and their composites and (c) DBzPBI-BuI, ZIF-8 and their composites.The ZIF-8 based composite mebranes show single stage degradation due tothe small defference between degradation temperatures of individual components: polymer and ZIF-8.

(c) Physical properties of composite membranes

Table S1. Density and mechanical properties of membranes with MOF loading

Membrane	% MOF (based on TGA char yield)	*Density (calculated) ($g.cm^{-3}$)	Density (experimental) ($g.cm^{-3}$)	Mechanical properties		
				Young Modulus (GPa)	Tensile strength (MPa)	Elongation at break (%)
PBI-BuI	-	-	1.193	4.2	131.2	26.1
Z_{10}@PBI-BuI	11.5	1.169	1.141	3.8	130.4	13.8
Z_{20}@PBI-BuI	18.1	1.144	1.113	3.5	129.7	5.0
Z_{30}@PBI-BuI	33.9	1.120	1.082	3.5	104.8	2.4
DMPBI-BuI	-	-	1.196	3.3	90.2	53.04
Z_{10}@DMPBI-BuI	9.2	1.171	1.122	3.2	94.9	15.5
Z_{20}@DMPBI-BuI	18.1	1.147	1.091	3.2	95.1	7.0
Z_{30}@DMPBI-BuI	27.6	1.122	0.965	3.0	65.4	2.3
DBzPBI-BuI	-	-	1.097	2.8	92.3	12.6
Z_{10}@DBzPBI-BuI	10.7	1.082	1.042	2.6	92.3	5.3
Z_{20}@DBzPBI-BuI	20.2	1.068	1.011	2.7	79.3	4.6

*Theoretical densities for composites were calculated using ZIF-8 densityas 0.95 $g.cm^{-3}$.[5]

(d) Gas permeation

(i) Instrumentation and method

The schematic of the permeability set up based on variable volume method is given in following Fig. S10. A feed side of the permeation cell was connected to the gas cylinder and a pressure transducer (0-550 psi range, accuracy: $\pm$ 0.1% over the full scale) through a 'T' joint and a valve 'V_1'. The vent valve 'V_2' was used for flushing and to control the feed pressure. On the permeate side of the 'permeation cell', the 'flow meter' was connected. It mainly consists a calibrated glass capillary of I.D. = 0.1 cm, containing a small mercury slug of ~ 0.5 cm in length. With the cathetometer (vertically travelling microscope), the readability of the flow meter is 0.005 cm.

The membrane cell assembly was kept in thermostat maintained at 35 °C. As a result of gas permeation, displacement of the mercury slug was monitored against time using cathetometer. The permeability (P) was calculated using the following equation.

$$P = \frac{F.C. \times d \times l}{\Delta p \times A \times t}$$

where, *'d'* = distance traveled by mercury slug (cm), *'F.C.'* = flow meter constant (volume of the flow meter capillary per unit length in cm^3/cm) *'l'* = thickness of the membrane (cm), *A* = effective membrane area (cm^2), *'t'* = time (sec), 'Δp' = pressure difference across the membrane (atm). The permeation measurements were repeated with at least 3 different membrane samples prepared under identical conditions and the data was averaged.

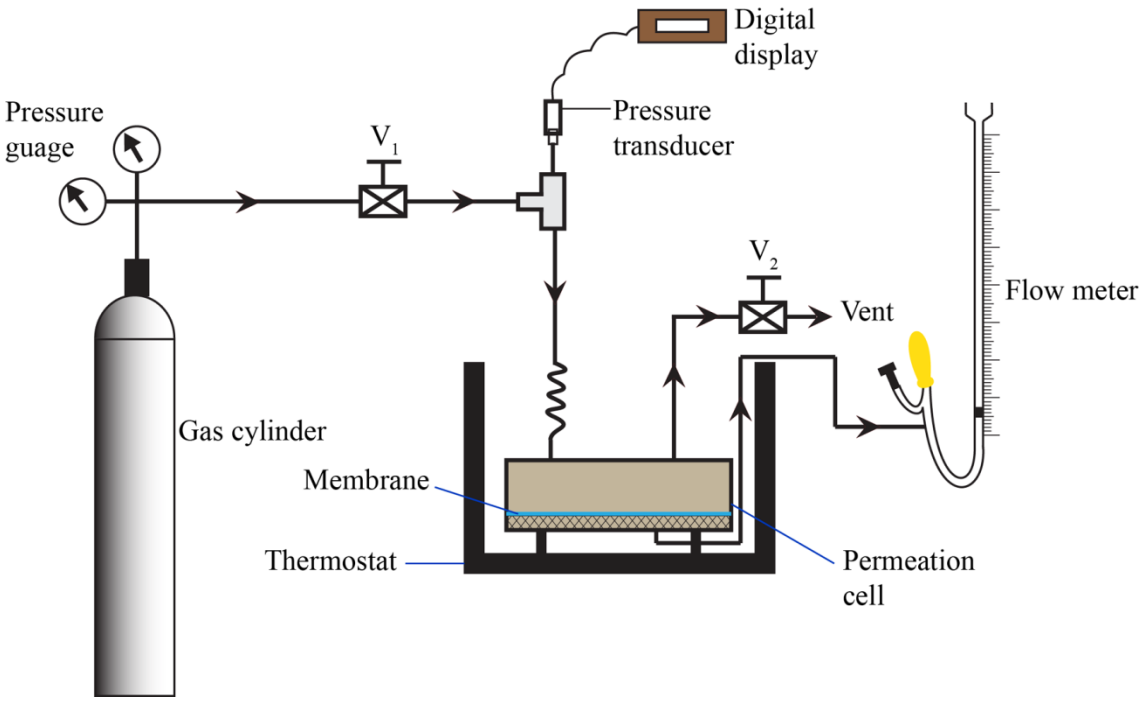

Fig. S7 Gas permeation assembly.

(ii) Gas permeation properties

Table. S2 Gas permeability coefficients (P)* and permselectivities (P_1/P_2) of ZIF-8 based composite membranes

	P_{He}	P_{H_2}	P_{N_2}	P_{CH_4}	P_{CO_2}	P_{He}/P_{N_2}	P_{H_2}/P_{N_2}	P_{He}/P_{CH_4}	P_{H_2}/P_{CH_4}	P_{H_2}/P_{CO_2}	P_{CO_2}/P_{N_2}	P_{CO_2}/P_{CH_4}
ZIF-8@PBI-BuI composite												
PBI-BuI	6.5	6.22	0.09	0.04	2.30	79.6	72.9	162.2	154.7	2.7	26.8	57.0
Z_{10}@PBI-BuI	11.6	11.37	0.14	0.05	2.80	83.9	82.0	225.6	220.4	4.1	20.2	54.2
Z_{20}@PBI-BuI	13.3	14.01	0.18	0.08	3.83	75.5	75.6	176.4	172.2	3.6	21.1	47.0
Z_{30}@PBI-BuI	21.6	22.11	0.33	0.12	5.23	65.6	67.3	179.5	184.1	4.2	16.0	43.6
ZIF-8@DMPBI-BuI composite												
DMPBI-BuI	11.0	12.8	0.18	0.08	3.8	61.9	72.1	135.1	157.5	3.4	21.7	47.2
Z_{10}@DMPBI-BuI	15.1	19.5	0.36	0.16	6.7	42.1	54.4	94.3	121.9	3.4	18.7	42.2
Z_{20}@DMPBI-BuI	29.9	37.8	0.64	0.28	9.0	46.9	59.3	106.2	134.3	3.8	14.0	31.4
Z_{30}@DMPBI-BuI	69.3	127.5	4.77	3.51	53.9	14.6	26.7	20.27	37.0	2.4	11.3	15.7
ZIF-8@DBzPBI-BuI composite												
DBzPBI-BuI	44.6	61.4	2.0	1.6	25.8	22.3	30.7	27.5	37.6	2.4	12.9	15.9
Z_{10}@DBzPBI-BuI	86.3	129.8	4.6	4.8	60.2	18.6	28.0	18.0	27.0	2.2	13.0	12.5
Z_{20}@DBzPBI-BuI	116.4	180.3	6.3	7.8	89.8	18.5	28.7	15.0	23.2	2.0	14.3	11.6

*Permeability coefficients are expressed in Barrer (1Barrer = 10^{-10} cm^3 (STP).cm/cm^2.s.cm Hg)

References

1. J. Cravillon, S. Mu¨nzer, S. J. Lohmeier, A. Feldhoff, K. Huber and M. Wiebcke, *Chem. Mater.,* 2009, 21*,* 1410.
2. S. C. Kumbharkar, P. B. Karadkar and U. K. Kharul, *J. Membr. Sci.,* 2006, **286**, 161.
3. S.C. Kumbharkar and U. K. Kharul,*Eur. Polym. J.*, 2009, **45,** 3363.
4. S. C. Kumbharkar and U. K. Kharul, *Polymer,* 2009, **50**, 1403.
5. Q. Song, S. K. Nataraj, M. V. Roussenova, J. C. Tan, D. J. Hughes, W. Li, P. Bourgoin, M. A. Alam, A. K. Cheetham, S. A. Al-Muhtasebd and E. Sivaniah, *Energy Environ. Sci.*, 2012, **5**, 8359.